International Journal for Research in Applied Science & Engineering Technology (IJRASET)
ISSN: 2321-9653; IC Value: 45.98; SJ Impact Factor: 7.177
Volume 7 Issue V, May 2019- Available at www.ijraset.com

Novel Approach on Stability Analysis of Single Phase Full Bridge Inverter with Reduced DC Link Capacitor

M.Karthika[1], Vinod Kumar S[2]
[1, 2]*Senior Assistant Professor, Department of EEE, New Horizon College of Engineering, Bangalore*

***Abstract:** This paper analyzes the stability of single phase full bridge converter with reduced dc link capacitance. The electrolytic capacitors are replaced by film capacitors which will increase the reliability of the system and decreases the capacitance. The conventional linear time-invariant (LTI) model may not represent the real converter behavior. This will lead to poor system performance or instability. Hence, the linear time-periodic (LTP) model is highly encouraged for stability and transient analysis. This paper also compares both LTP and LTI model by considering the control gain and dc-bus capacitance size. The stability is analyzed using an Atmega 328 microcontroller. For any of these cases, the Linear Time Periodic (LTP) model are highly encouraged for stability and transient analysis as a tool for controller design.*

I. INTRODUCTION

Most of power electronic converters have been used in low-cost single-phase applications, where price constraints are a highly relevant issue. Single-phase ac/dc converters have pulsating input energy conversion, which produces some low- order non-characteristic harmonics in the dc-link [1]. In order to obtain a regulated output voltage, these converters normally include bulky electrolytic dc-link capacitors to filter out low-frequency voltage ripple.

In recent years, one important trend in the design of ac/dc converters has been to increase their lifetime. Since electrolytic capacitors reduce system reliability because of short lifetime, their replacement by long lifetime film capacitors has been considered in many cases [4]. However, as film capacitors have lower power density and higher cost, and many designs have been done with small dc-link capacitance. PFC ac/dc converters with small dc-link capacitance have low stored energy in dc- link[7,8]. In these cases, fast dynamic response dc-link voltage control must be used in order to avoid a significant dc-link voltage fluctuation due to abrupt load changes.

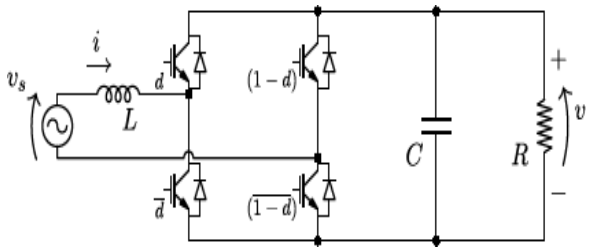

Fig.1: Circuit diagram

Consider the single phase ac-dc full-bridge converter with power factor correction (PFC) shown in Fig1. The converter has four switches, where the input inductor L reduces input current ripple and the output capacitor C reduces dc link voltage 100/120Hz ripple. A sinusoidal PWM technique is used to obtain the switch signals by modulating the duty cycle[9,10]. The output is connected to a resistive load R, while the single-phase grid v_S is considered a low impedance sinusoidal source.

II. PROPOSED TOPOLOGY

Several design techniques have been presented to improve the dc-link voltage dynamic response of single-phase PFC converters without compromising the input power factor (PF).However, the combination of fast dynamic response ac/dc dc-link voltage control with small dc-link capacitance may lead to poor system performance and instability. This occurs due to interactions of dc-link low frequency voltage ripple with the feedback control loop.

International Journal for Research in Applied Science & Engineering Technology (IJRASET)
ISSN: 2321-9653; IC Value: 45.98; SJ Impact Factor: 7.177
Volume 7 Issue V, May 2019- Available at www.ijraset.com

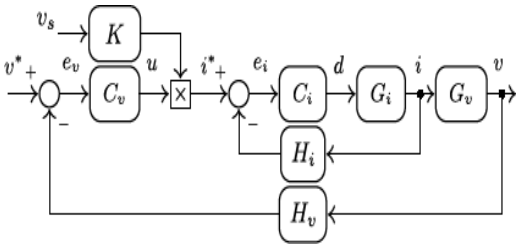

Fig.2: Closed loop control block diagram.

The input-output frequency conversion which occurs in PFC converters is suitably described by the modulation theory. Linear time periodic (LTP) models are suitable to describe such dynamic systems, since it models the frequency modulations and is suitable to analyze the spectral interactions due to the feedback. Analogous to Laplace transfer functions (TF), the LTP systems can be represented in the frequency- domain by Harmonic Transfer Functions (HTF).

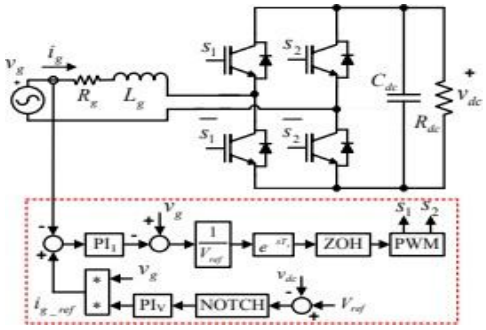

Fig.3: Schematic and control of proposed topology HTF modeling methodology is based on the linear independence of the exponential terms of the model, well know under Exponentially Modulated Signal (EMP) theory. HTF models can be used to design the controller as well as to analyze the stability using the generalized Nyquist criterion.

This paper proposes to investigate the stability of an ac-dc full-bridge converter with power factor correction with reduced dc-link capacitance considering both conventional LTI and LTP approaches. Complete LTI and LTP models are presented on the frequency-domain, and the stability is analyzed considering both approaches. Also, a design example is presented of an ac-dc full-bridge converter with reduced dc-link capacitance and high- frequency outer voltage loop bandwidth. Experimental validation demonstrates that the LTP approach accurately models the converter stability.

S.NO	Parameter	Ratings
1	Nominal input voltage VRMS	127 V
2	Output voltage V	300 V
3	Nominal output power Po	375 W
4	Input inductor L	560H
5	DC capacitor C	680F
6	Load resistance R	240 ohm
7	Switching/Sampling frequency Ts	46875 Hz
8	Direct input voltage gain K	1=(127/p 2) A/V
9	Feedback voltage gain Hv	1
10	Feedback current gain Hi	1

Table.1: Converter Parameters and Nominal Specification

A conventional PFC control structure of ac-dc full-bridge converter is shown in Fig3. This control schemes is based on two control layers: an inner current loop to ensure a sinusoidal input current waveform, and an outer voltage loop for dc-link voltage regulation. The outer loop compensator Cv regulates the average dc voltage v by calculating the magnitude of current reference u. Power factor correction is achieved from voltage vs by: i_(t) = Kvs(t)u(t) (1)(1)
where i is the current reference and has the same shape of vs. Additionally, the duty- cycle d is the control action of the inner loop compensator Ci to make the current i track its reference i. The blocks Gi and Gv denote the current i and voltage v plants, respectively. The sensor gains Hi and Hv are also illustrated for current and voltage measures, respectively. Disregarding the modulation frequency fs and their harmonic components, the model for the full-bridge are obtained for averaged values in the switching period Ts. In this way, all measured values are written in terms of the averaged input voltage, defined as:---(2)

$$v_s(t) = \frac{1}{T_s}\int_t^{t+T_s} v_{in}(\tau)\, d\tau$$

Then, since the control action d is defined in the interval [0, 1], the non-linear model state equation takes a well known form.---------(3)

$$\begin{bmatrix}\dot{i}(t)\\ \dot{v}(t)\end{bmatrix} = \begin{bmatrix}0 & \frac{1-2d(t)}{L}\\ \frac{2d(t)-1}{C} & \frac{-1}{RC}\end{bmatrix}\begin{bmatrix}i(t)\\ v(t)\end{bmatrix} + \begin{bmatrix}\frac{1}{L}\\ 0\end{bmatrix} v_s(t)$$

A. Open-Loop LTP Small Signal Model

In the control structure of Fig.3 the current reference I is a time-periodic function, and then, its behavior should be included in the LTP model. This implies that the inner current loop should be also included in the open-loop small signal model. Thus, the presented LTP model describes the perturbation behavior from u to v. Since the current control is a LTI state-space equation that defines the duty-cycle d based on the current error ei, given by:

x_i(t) = Aixi(t) + Biei(t)---------- (4)

d(t) = Cixi(t) + Diei(t) ---------- (5)

where the current error ei(t) = Kvs(t)u(t)
Hii(t) is determined by the control scheme. The full-bridge complete model from u to v are, then, determined by replacing the output current control function and the current control states xi of are included to non-linear full-bridge model .Then, can be written

$$\begin{aligned}\dot{x}_i(t) &= A_i x_i(t) - B_i H_i i(t) + B_i K v_s(t) u(t)\\ \dot{i}(t) &= -\frac{1}{L}v(t) - \frac{2C_i}{L}x_i(t)v(t) + \frac{2D_i H_i}{L}i(t)v(t) +\\ &\quad -\frac{2D_i K}{L}v_s(t)v(t)u(t) + \frac{1}{L}v_s(t)\\ \dot{v}(t) &= -\frac{1}{RC}v(t) + \frac{2C_i}{C}x_i(t)i(t) - \frac{2D_i H_i}{C}i^2(t) +\\ &\quad -\frac{1}{C}i(t) + \frac{2D_i K}{C}v_s(t)i(t)u(t)\end{aligned}$$

-----(6)

The linear-time version of is determined by applying a perturbation signal around the nominal value for each variable. The biggest difference between LTI and LTP methodology is that LTP has time varying nominal values, typically sinusoidal. In this way, the current control states are xi(t)
= Xi(t)+ ~ xi(t), the input current i(t) = I(t)+~i(t), the output voltage v(t) = V + ~v(t), the voltage control action u(t) = U + ~u(t), and the input voltage vs(t) = Vs(t) + ~vs(t) are replaced . Where the capitalized variables are steady-state functions and the perturbation signals are denoted by~sign. Additionally, the nominal steady-state averaged input voltage stands over one switching period Ts (2), and can be expressed by:---(7)

$$V_s(t) = \sqrt{2}V_{RMS}[\epsilon_1 \sin(\omega_1 t) + \epsilon_2 \cos(\omega_1 t)]$$

$$\epsilon_1 = \frac{(\cos(\omega_1 T_s) - 1)}{\omega_1 T_s}$$

$$\epsilon_2 = \frac{\sin(\omega_1 T_s)}{\omega_1 T_s}$$

Replacing the averaged steady-state functions and simplifying the quadratic and non-linear terms of perturbation signals the following linear-time periodic state-space equation can be obtained:--(8)

$$\begin{bmatrix} \dot{\tilde{x}}_i(t) \\ \dot{\tilde{i}}(t) \\ \dot{\tilde{v}}(t) \end{bmatrix} = \begin{bmatrix} A_i & -B_i H_i & 0 \\ \frac{-2VC_i}{L} & \frac{2VD_i Hi}{L} & \gamma_1(t) \\ \gamma_2(t) & \gamma_3(t) & \frac{-1}{RC} \end{bmatrix} \begin{bmatrix} \tilde{x}_i(t) \\ \tilde{i}(t) \\ \tilde{v}(t) \end{bmatrix} +$$

$$+ \begin{bmatrix} \gamma_4(t) & \frac{V^2 B_i H_i}{RV_{RMS}} & 0 \\ \gamma_5(t) & \frac{1}{L}\left(1 - \frac{2V^3 D_i H_i}{RV_{RMS}}\right) & 0 \\ \gamma_6(t) & \gamma_7(t) & 1 \end{bmatrix} \begin{bmatrix} \tilde{u}(t) \\ \tilde{v}_s(t) \\ \gamma_8(t) \end{bmatrix}$$

which time-varying coefficients n(t) are strictly periodic, given by:

$$\gamma_1(t) = \delta_1 \sin(\omega_1 t) + \lambda_1 \cos(\omega_1 t)$$

$$\delta_1 = \frac{-1}{L}\left(\frac{\sqrt{2}\omega_1 LV}{RV_{RMS}}\epsilon_2 + \frac{\sqrt{2}V_{RMS}}{V}\epsilon_1\right)$$

$$\lambda_1 = \frac{1}{L}\left(\frac{\sqrt{2}\omega_1 LV}{RV_{RMS}}\epsilon_1 - \frac{\sqrt{2}V_{RMS}}{V}\epsilon_2\right)$$

$$\gamma_2(t) = \delta_2(\epsilon_1 \sin(\omega_1 t) + \epsilon_2 \cos(\omega_1 t))$$

$$\delta_2 = \frac{2\sqrt{2}C_i V^2}{RCV_{RMS}}$$

---(10)

$$\gamma_6(t) = k_6 + \delta_6 \sin(2\omega_1 t) + \lambda_6 \cos(2\omega_1 t)$$
$$k_6 = \frac{2D_i K V^2}{RC}(\epsilon_1^2 + \epsilon_2^2)$$
$$\delta_6 = \frac{2\sqrt{2}D_i K V^2}{RCV_{RMS}}\epsilon_1\epsilon_2$$
$$\lambda_6 = \frac{2D_i K V^2}{RC}(\epsilon_2^2 - \epsilon_1^2)$$
$$\gamma_7(t) = \delta_7(\epsilon_1 \sin(\omega_1 t) + \epsilon_2 \cos(\omega_1 t))$$
$$\delta_7 = \frac{2\sqrt{2}D_i H_i V^4}{CR^2 V_{RMS}^3}$$
$$\gamma_8(t) = k_8 + \delta_8 \sin(2\omega_1 t) + \lambda_8 \cos(2\omega_1 t)$$
$$k_8 = \frac{V}{RC}(\epsilon_1^2 + \epsilon_2^2 - 1)$$
$$\delta_8 = \frac{1}{C}\left(\frac{\omega_1 L V^3}{R^2 V_{RMS}^2}(\epsilon_2^2 - \epsilon_1^2) + \frac{2V}{R}\epsilon_1\epsilon_2\right)$$
$$\lambda_8 = \frac{1}{C}\left(\frac{-2\omega_1 L V^3}{R^2 V_{RMS}^2}\epsilon_1\epsilon_2 + \frac{V}{R}(\epsilon_2^2 - \epsilon_1^2)\right)$$

--(11)

B. Simplified Open-Loop LTP Small- Signal Model

Most design techniques assume that the current-loop is designed with a bandwidth ten times faster or more than the bandwidth of voltage-loop. This dynamically decouples current and voltage control loops, with makes possible to independently design both controllers. Additionally, to ensure the PFC issue, a sinusoidal internal model is normally added to the current loop to track as close as possible the current reference. Under this assumption, for voltage loop, the current can be considered as:

$$i(t) = \frac{1}{H_i} i^*(t) = \frac{K}{H_i} v_s(t) u(t)$$

---(12)

In addition, the current state i may be used to determine the duty-cycle for the voltage state v, given by:

$$d(t) = \frac{1}{2} + \frac{v_s(t)}{2v(t)} - \frac{L\dot{i}(t)}{2v(t)}$$

----(13)

Whether current and voltage control loops are dynamically decoupled, than normally a higher switching frequency is also applied. Since the switching frequency is forty times faster than the fundamental input voltage frequency
Furthermore, this condition simplifies the averaged input voltage, which results in:

$$V_s(t) = \sqrt{2}V_{RMS}\cos(\omega_1 t)$$
$$v(t)\dot{v}(t) = \frac{-1}{RC}v^2(t) + \frac{1}{C}v_s(t)i(t) - L\dot{i}(t)i(t)$$

--(14)

Then, applying the perturbation signal around the steady-state condition, and simplifying the second order and non- linear terms of perturbation, results in the following simplified LTP model given by

$$\dot{\tilde{v}}(t) = \frac{-2}{RC}\tilde{v}(t) + \begin{bmatrix}\phi_1 & \phi_2 & 1\end{bmatrix}\begin{bmatrix}\tilde{u}(t)\\ \tilde{v}_s(t)\\ \phi_3(t)\end{bmatrix}$$

$$\phi_1(t) = \frac{KV_{RMS}^2}{H_i VC} + \frac{KV_{RMS}^2}{H_i VC}\cos(2\omega_1 t) + \frac{2LVK\omega_1}{H_i RC}\sin(2\omega_1 t)$$

$$\phi_2(t) = \frac{2\sqrt{2}V}{RCV_{RMS}}\cos(\omega_1 t) + \frac{\sqrt{2}LV^3\omega_1}{R^2CV_{RMS}^3}\sin(\omega_1 t)$$

$$\phi_3(t) = \frac{V}{RC}\cos(2\omega_1 t) + \frac{LV^3\omega_1}{R^2CV_{RMS}^2}\sin(2\omega_1 t)$$

The origin of an output harmonic of frequency when a dc input is applied is named frequency shifting. The LTI model that relates the control action disturbance
~u to the output voltage ~v can be directly determined from disregarding its sinusoidal terms, which results in the following:

$$G_v(s) = \frac{\tilde{V}(s)}{\tilde{U}(s)} = \left(\frac{KV_{RMS}^2}{H_i VC}\right)\frac{1}{s + \frac{2}{RC}}$$

C. Stability Analysis: Linear-Time Invariant Case

The LTI stability analysis approach is used when the converter is represented by the average LTI model. The stability analysis in frequency domain has been done using the Nyquist criterion represented in Fig. 4, which is the eigenloci contour of the open- loop equation HvCv(s)Gv(s) calculated for the path shown in Fig4. The graphical interpretation indicates a stable closed- loop behavior, because the eigenloci contour does not encircles the point (1 + j0).The calculated GM=10.84=20.7dB @2_98 rad/s and the PM=49°@2_38 rad/s.

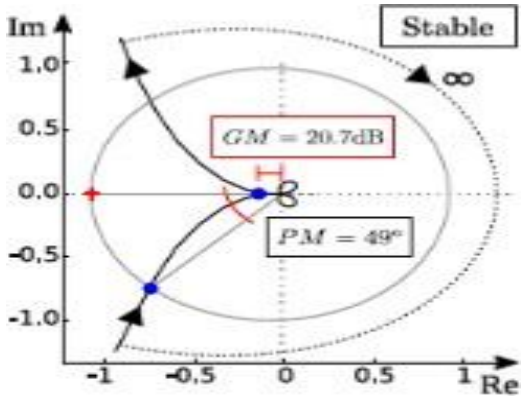

Fig.4.Stability Analysis: Linear-Time Periodic Case

III. EXPERIMENTAL RESULTS

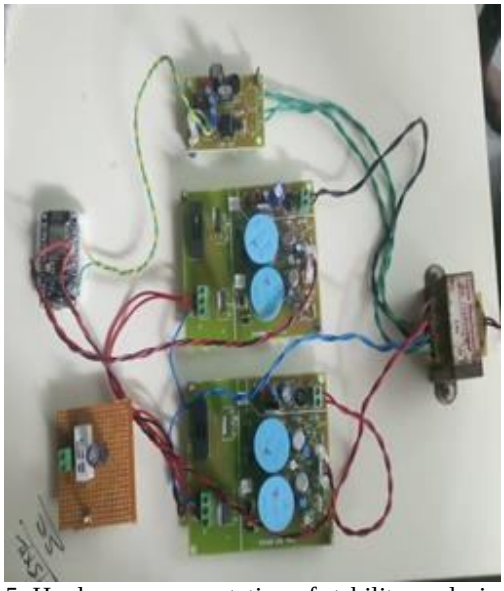

Fig.5: Hardware representation of stability analysis

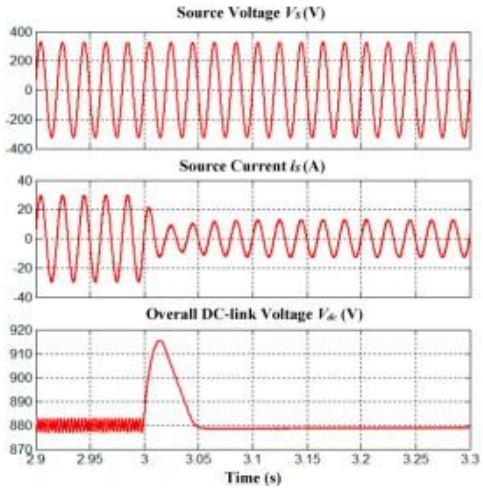

Fig.6:Simulation results

IV. CONCLUSION

The stability analysis and dynamic response of a DC-link module with a series voltage compensator theoretical analysis reveals that a stable operation can be achieved with the proposed DC-link module from both power flow perspective and impedance perspective. For experimental validations, a DC-link module is built for a 600W AC-DC-DC test bed, which achieves 82% reduction of the DC-link capacitance and more than 8 times lifetime extension of the DC-link capacitors. The experimental results of steady-state operation, start-up, and step- up and step-down load reveals that the proposed DC-link module retain the control performance compared to that of conventional E-Caps solution in terms of both stability and dynamic responses.

In this paper, it was demonstrated that the stability of dc-link outer voltage loop of PFC ac-dc converters may not be always well stated by conventional LTI models. Also it was shown that LTP models represent the converter's dynamics better way since it includes the converter sinusoidal modulation and harmonic interactions. The results we have presented may assist in the design of the control system of PFC ac-dc converters when small dc-link capacitance is used or a fast voltage dynamic response is necessary. This is important to increase lifetime and enhance performance of these converters.

REFERENCES

[1] Garcia, M. Rico, J. Sebastian, M. M. Hernando, J. Uceda, "An optimized DC-to-DC converter topology for high- voltage pulse-load applications", IEEE Power Electronics Specialists Conference, vol. 2, pp. 1413-1421.
[2] M. di Bernardo, F. Vasca, "Discrete- time maps for the analysis of bifurcations and chaos in DC/DC converters", Circuits and Systems I: Fundamental Theory and Applications IEEE Transactions on, vol. 47, pp. 130-143, 2000.
[3] Z. Zhe, O. C. Thomsen, M. A. E.Andersen, J. D. Schmidt, H. R. Nielsen, "Analysis and Design of Bi-directional DC-DC Converter in Extended Run Time DC UPS System Based on Fuel Cell and Supercapacitor", Applied Power Electronics Conference and Exposition 2009. APEC 2009, pp. 714-719, 2009
[4] Connected Converters Basic Criteria in Designing LCL Filters for Grid Connected Converters" , IEEE ISIE 2006, July 9-12, 2006, Montreal, Quebec, Canada.
[5] Karshenas, H.R.; Saghafi, H., "Performance Investigation of LCL Filters in Grid Connected Converters," Transmission & Distribution Conference and Exposition: Latin America, 2006. TDC '06. IEEE/PES , vol., no., pp.1,6, 15- 18 Aug. 2006
[6] P. Daly and J. Morrison," Understanding the Potential Benefits of Distributed Generation on Power Delivery," IEEE Rural Electric Power Conference, 2001
[7] M. Liserre, F. Blaabjerg, and S.Hansen "Design and Control of an LCL-Filter- Based Three-Phase Active Rectifier," IEEE Trans. Industry Applications, vol. 41, no. 5, pp. 1281-1291, September/October 2005
[8] J. C. Wu and H. L. Jou, "A new UPS scheme provides harmonic suppression and input power factor correction," IEEE Trans. Ind. Electron., vol. 42, no. 6, pp. 629–635, Dec. 1995.
[9] P. K. Jain, J. R. Espinoza, and H. Jin, "Performance of a single-stage UPS system for single-phase trapezoidal-shaped ac-voltage supplies," IEEE Trans. Power Electron., vol. 13, no. 5, pp. 912–923, Sep. 1998.
[10] Xiao-Qiang Li, Xiao-Jie Wu, Yi-Wen Geng, and Qi Zhang; "Stability Analysis of Grid-Connected Inverters with an LCL Filter Considering Grid Impedance", Journal of Power Electronics, Vol. 13, No. 5, September 2013
[11] Sze Sing Lee, Bing Chu, NikRumzi NikIdris, Hui Hwang Goh, Yeh En Heng, "Switched-Battery Boost-Multilevel Inverter with GA Optimized SHEPWM for Standalone Application", IEEETrans. Ind. Electron., vol. 63, no. 4, pp. 2133-2142, 2016
[12] Y. Xia, R. Ayyanar, "Adaptive Dc Link Voltage Control Scheme for Single Phase Inverters with Dynamic Power Decoupling", 2016 IEEE Energy Conversion Congress and Exposition (ECCE), pp. 1-6, 2016.
[13] L. Cong, H. Lee, "High-voltage high- frequency non-isolated multiphase DC-DC converters with passive-saving two-phase QSW-ZVS technique", Journal of Analog Integrated Circuits and Signal Processing, vol. 88, no. 2, pp. 303-317, Aug. 2016.
[14] V. K. Devi, S. Srivani, "Modified phase shifted PWM for cascaded H bridge multilevel inverter", Advances in Electrical Electronics Information Communication and Bio-Informatics (AEEICB) 2017 Third International Conference on, pp. 89-94, 2017